DARTMOUTH COLLEGE

Thayer School of Engineering

Hanover, New Hampshire

MAGNETOPAUSE STRUCTURE DURING THE MAGNETIC STORM OF SEPTEMBER 24, 1961.

BENGT U.Ö. SONNERUP

JULY 1970

This work was supported by National Aeronautics and Space Administration under Grants NGR-30-001-011 and NGR-30-002-010 with University of New Hampshire

MAGNETOPAUSE STRUCTURE DURING THE MAGNETIC STORM OF SEPTEMBER 24, 1961.

BENGT U.Ö. SONNERUP

JULY 1970

This work was supported by National Aeronautics and Space Administration under Grants NGR-30-001-011 and NSG-624.

Abstract

An account is given of the Explorer 12 magnetic field observations of the magnetopause current layer on the inbound pass of Sept. 24, 1961, which occurred during the main phase of a moderately strong magnetic storm. The accuracy of the Explorer 12 data reported here has been increased by use of an improved filtering procedure. Five magnetopause penetrations were observed in a time period of about 20 minutes and for each of these the data were used to calculate the vector normal to the current layer, the magnetic field component along that vector and the polarization of the current layer. Normal magnetic-field components significantly different from zero were obtained and it is suggested that the observations during this pass in general are consistent with the so-called open magnetosphere model. In fact, it appears that the first and the last of the boundary penetrations may have occurred on opposite sides of, but very near, the X-type magnetic null line which is located on the front side of the open magnetosphere model. The direction of the normal magnetic-field component as well as the sense of polarization of the current layer were found to be opposite for these two boundaries.

Introduction

It is the purpose of this report to present the magnetometer data from a set of Explorer 12 magnetopause penetrations during the inbound pass of Sept. 24, 1961, when a moderate magnetic storm was in progress, and to propose an interpretation of these data in terms of the so-called open magnetosphere model (Dungey, 1961).

The magnetometer experiment onboard Explorer 12 has been described in some detail by Cahill and Amazeen (1963). Approximately three complete field-vector measurements were obtained per second. All Explorer 12 magnetometer data published to date were obtained by passing the analog output from each of the three fluxgate magnetometers through a set of digital filters with a window size of approximately 24γ. The data presented here were obtained by instead passing the original telemetry tapes through an improved filter line yielding data that for the purposes of this paper can be considered to be in analog form. While in most cases where this improved reduction procedure was attempted the Explorer 12 data was too noisy to make the procedure worthwhile, the data from Sept. 24, and a few other days, appeared greatly improved with a substantial reduction in noise level, compared to the digital data. Thus the Explorer 12 magnetopause records presented here are considered to be substantially better than those used in previous analyses (Sonnerup and Cahill, 1967, 1968). An indication of the accuracy of the data is obtained from the zero-level corrections for the two magnetometers measuring the field perpendicular to the spin axis. These corrections

were found to be -2.4γ and -.3γ for the X and Y magnetometers, respectively, for the Sept. 24 event.

The details of the Explorer 12 orbit can also be found in the paper by Cahill and Amazeen (1963). The five magnetopause crossings to be discussed here occurred in the time interval 19.21 - 19.40 UT. The satellite location during this interval is given in Table 1. It is seen that the satellite was located near the 'nose' of the magnetosphere, a few degrees over on the morningside but almost exactly in the so-called solar-magnetospheric equatorial plane, i.e., the plane through the earth's center that is perpendicular to the plane containing the solar-wind velocity vector and the geomagnetic dipole axis. An abberation of 5° of the former vector from the antisolar direction is assumed. It is seen from Table 1 that at 19.21 UT the satellite was about 0.3° on the southern side of the solar-magnetospheric equatorial plane while at 19.40 it was about 0.6° on the northern side of that plane.

A magnetic storm of moderate strength was in progress on Sept. 24, 1961. The magnetopause observations to be presented here occurred during the main phase of that storm. The 3-hour K_p index for the period in question was $K_p = 5$. Magnetograms from several low and mid-latitude stations are shown in Fig. 1.

Table 1. Satellite Position

R_p/R_E is the geocentric distance in earth radii, θ_p and ϕ_p are the geomagnetic colatitude and longitude, respectively. The former is < 90° in the northern hemisphere, the latter is counted positive west from the plane containing the solar-wind vector and the dipole axis. Thus $\phi_p = 0$ at the 'nose' and $\phi_p > 0$ on the morning side of the magnetosphere.

Time, UT	Satellite Position			Solar-Wind Velocity	
	R_p/R_E	θ°_p	ϕ°_p	θ°_{sw}	ϕ°_{sw}
19.21	8.9	80.8	9.0	99.5	180
19.40	8.5	80.6	7.9	98.8	180

Data presentation

Figures 2a - 2d show survey plots of the Explorer 12 magnetometer records for the period 19.15 - 19.46 UT on Sept. 24, 1961. The magnetic field vector is represented in a spherical polar coordinate system (B, α, ψ) with the polar axis along the satellite spin axis. At 19.28 UT the latter has geomagnetic colatitude $\theta_{sp} \cong 132°$ and longitude $\phi_{sp} \cong 129°$ with the angles θ and ϕ defined in Table 1. The angles α and ψ are the polar angle and the azimuth angle, respectively. The former is equal to zero when the field vector points along the positive spin axis, the latter is zero when the field lies in the plane containing the spin axis and the sun direction and points towards the sun. Also, ψ is equal to 90° and 270° when the field is due north and south, respectively. This coordinate system was described in detail by Cahill and Amazeen (1963). It has been used in the presentation of much of the Explorer 12 magnetometer data.

Magnetopause crossings are observed as a large change in the angle ψ usually accompanied by a change in the angle α and in the field magnitude B. Examination of Fig. 2a shows the following: The satellite is initially in the transition zone with $\psi \simeq 300°$, $\alpha \simeq 60°$. Large periodic field-magnitude variations, presumably associated with fast or slow MHD waves are seen. The wave period appears to be 60 - 70 sec. In Fig. 2b the first entry into the magnetosphere is observed at approximately 19.21 UT. The angles ψ and α take on the values ~135°

and ~ 115°, respectively. The field magnitude is generally higher than in the transition zone but it is noted that large periodic field-magnitude variations with a period of 40-50 sec. are present also on the magnetosphere side of the magnetopause. It appears reasonable to assume that these are waves which originated somewhere in the transition zone and were transmitted across the magnetopause. Alternatively they could be interpreted as field structures convected across the magnetopause of an open magnetosphere.

At approximately 19.25.30 UT the satellite again appears to leave the magnetosphere for a brief time period. The angles ψ and α show a tendency to return to the values representative of the transition zone. However, the field intensity is lower than that seen in Fig. 2a. At 19.26 UT the satellite has returned into the magnetosphere and B, α, ψ have taken on about the same values as before. At 19.27.30 UT the satellite again leaves the magnetosphere and stays in the transition zone (Fig.2c) until 19.38 UT when it gradually reenters (Fig. 2d) over a period of several minutes. At about 19.45 UT the angles ψ and α have again taken on the values 135° and 115°, respectively. The 19.38 UT boundary is the last (i.e., innermost) boundary observed on this pass. Thus it is reasonably clear that these values of ψ and α represent the magnetospheric field just inside the magnetopause. The fact that these angles also occur during the time intervals 19.21 - 19.25.30 UT and 19.26 - 19.27.30 UT suggests that the interpretation of the boundaries at 19.21,

19.25.30, 19.26 and 19.27.30 UT as true magnetopause penetrations is likely to be correct.

The energetic proton and electron observations (Davis and Konradi, 1968) during the period of interest are not presented in detail here. However, it is noted that protons at a reduced flux level first appear at about 19.16 UT and are then observed during the entire period 19.16 - 19.45 UT. At about 19.45 - 19.50 UT the proton flux level increases to a value representative of the outer magnetosphere. Except for a brief spike at about 19.24 UT energetic electrons are not seen until 19.45 UT when they abruptly take on magnetospheric flux levels. These observations are in harmony with the interpretation of the five events mentioned above as true magnetopause penetrations, provided that the first two satellite reentries into the magnetosphere did not bring the satellite into the region of high particle fluxes.

In the survey plot of Fig. 2 the data is presented in the form of continuous averages, each taken over 16 individual field measurements. Thus the time separation between neighboring points in Fig. 2 is approximately 5 sec. Also the old (digital) data was used for this plot. All subsequent figures in this paper are based on the improved data.

Figures 3 - 7 show the five individual boundary crossings in detail. In these figures each individual data point is shown so that the time separation between neighboring points is .327 sec. It is seen that the durations of the first four magnetopause

crossings are of the order of 10 seconds. As pointed out before, the duration of the last crossing is considerably longer. Figure 7 shows only that segment of the total crossing where the field-direction change takes place reasonably rapidly. The nature of the impulsive field variation in Fig. 7 at 19.37.45 UT is not known. It may be a wave packet of some type travelling through the magnetopause. Alternatively, it may be a magnetic field structure that convected across the magnetopause with the transition-zone plasma.

The magnetometer data from the time intervals denoted by Δt in Figures 3 - 7 have been used for a minimum-variance analysis of the type described by Sonnerup and Cahill, (1967). In other words, the eigenvectors $\underset{\sim}{n}_1$, $\underset{\sim}{n}_2$ and $\underset{\sim}{n}_3$ and the corresponding eigenvalues λ_1, λ_2 and λ_3 of the matrix

$$M_{\alpha\beta} = (\overline{B_\alpha B_\beta} - \overline{B}_\alpha \overline{B}_\beta) \qquad \alpha,\beta = 1, 2, 3$$

have been determined. Here B_α and B_β are the Cartesian components of an individual measured field vector and the overhead bar denotes an average over all measured vectors in the time interval Δt. It is noted that an individual eigenvalue represents the variance of the magnetic field component along the corresponding eigenvector and that in a one-dimensional stationary magnetopause model the direction perpendicular to the magnetopause current layer is given by the eigenvector $\underset{\sim}{n}_1$, corresponding to the smallest eigenvalue λ_1.

The resulting eigenvalues and eigenvectors are given in Table 2. It is seen that for all boundaries the ratio λ_2/λ_1

of the intermediate to the smallest eigenvalue is larger than about three. Thus, the variance ellipsoids are nondegenerate and in each case $\underset{\sim}{n}_1$ should give an accurate estimate of the direction perpendicular to the magnetopause, provided that the structure of the latter is approximately one-dimensional, and provided that its attitude does not change significantly during the satellite penetration time.

The data in Table 2 shows that relatively large changes in the magnetopause attitude take place between the individual penetrations. Thus, it is difficult to obtain a reliable normal direction if the penetration time is of the order of minutes as in the case of the 19.40 UT boundary. For this reason only the time segment Δt in Fig. 7 around 19.38 UT in which the most rapid field changes of this boundary take place has been analyzed by the minimum-variance method. An earlier calculation (Sonnerup and Cahill, 1967) of the boundary normal on this occasion utilized 20 minutes of data. It yielded a normal direction given by $\theta = 69°$ $\phi = 3°$ and a normal field component of -2γ. This result is now considered to be in error. The vector normal to the 19.27.30 UT boundary was also reported earlier as $\theta = 72°$ $\phi = 3°$ with a normal-field component of -7γ. The old calculation utilized 90 and 160 individual field vector measurements while only 50 such measurements were used in the present calculation. The new calculation should be considered more reliable.

Table 2. Eigenvalues and Eigenvectors of $M_{\alpha\beta}$

The eigenvectors are given in terms of the geomagnetic colatitude θ and longitude ϕ. These angles* are defined in Table 1. The theoretical normal vector has $\theta_t = 80.7°$, $\phi_t = 5.5°$.

Time UT		λ $(\gamma)^2$	Direction Geomagnetic $\theta°$	$\phi°$	$\underline{B} \cdot \underline{n}$ (γ)
	$\underset{\sim}{n}_1$	82	71	30	- 8.0
19.21.00	$\underset{\sim}{n}_2$	242	95	118	12.7
	$\underset{\sim}{n}_3$	5642	19	-166	- 4.2
	$\underset{\sim}{n}_1$	13	77	- 4	- 6.3
19.25.30	$\underset{\sim}{n}_2$	71	73	90	- .7
	$\underset{\sim}{n}_3$	1465	22	-129	35.5
	$\underset{\sim}{n}_1$	21	78	11	- 3.2
19.26.00	$\underset{\sim}{n}_2$	107	103	98	-15.0
	$\underset{\sim}{n}_3$	1528	18	143	40.3
	$\underset{\sim}{n}_1$	27	69	- 3	2.5
19.27.30	$\underset{\sim}{n}_2$	171	93	85	-21.1
	$\underset{\sim}{n}_3$	3733	21	167	23.5
	$\underset{\sim}{n}_1$	24	65	- 10	26.7
19.38.00	$\underset{\sim}{n}_2$	100	69	90	-64.5
	$\underset{\sim}{n}_3$	1101	34	-145	12.9

* All angles were transformed from satellite coordinates to geomagnetic coordinates by use of the satellite position at 19.28 UT.

With the old (digital) Explorer 12 data the tendency for the minimum-variance direction to lie along the satellite spin axis seriously hampered the use of the minimum-variance method for the determination of the vector normal to the magnetopause (Sonnerup and Cahill, 1967). In that case the spin modulation of the outputs from the two magnetometers with axes perpendicular to the satellite spin axis and the absence of spin modulation of the spin-axis magnetometer led to a nonisotropic addition of the digital noise and an associated distortion of the true variance ellipsoid. This type of difficulty does not arise with the improved (analog) data provided that care has been taken to eliminate the zero-level errors of the magnetometers measuring the field perpendicular to the spin axis. As pointed out in the introduction, the zero-level errors appeared to be small during the Sept. 24 event. Nevertheless, these errors were removed.

The normal vectors $\underset{\sim}{n}_1$ in Table 2 may be compared with a theoretical normal vector $\underset{\sim}{n}_t$ for this time period, obtained from the Mead-Beard magnetosphere model (see Sonnerup and Cahill, 1967). This vector has $\theta_t = 80.7°$, $\phi_t = 5.5°$. It is seen that there are in general rather large angular deviations of the measured normal vector $\underset{\sim}{n}_1$ from the theoretical one.

Figures 8 - 12 show polar plots of the magnetic field component tangential to the magnetopause during the five penetrations discussed here. An arrow from the origin to an individ-

ual point represents the tangential-field component of one individual field-vector measurement. The two axes shown in these diagrams are the $\underset{\sim}{n}_2$ and $\underset{\sim}{n}_3$ directions given in Table 2. The vectors $\underset{\sim}{n}_2$ and $\underset{\sim}{n}_3$ are due roughly west and north, respectively. It is noted from these figures that the polarization of the magnetopause appears to change in the time interval 19.21 - 19.38 UT. In other words, an observer moving outwards from the earth through the magnetopause would find that at 19.21 UT the tangential magnetic field vector rotates in the right-hand sense when seen from the earth while a similar penetration at 19.38 UT would yield a left-hand rotation. For the intermediate crossings the sense of rotation is indeterminate. A possible interpretation of this observation will be presented in the discussion section.

Figure 13 shows the variation of the magnetic field component along $\underset{\sim}{n}_1$, i.e., along the calculated normal direction. In a one-dimensional steady magnetopause model this field component should remain constant in order to assure that $\underline{\nabla} \cdot \underline{B} = 0$. It is seen that the individual field measurements may deviate substantially from the average value. In particular this is the case for the 19.21 UT boundary. The deviations appear to be more or less random. It is noted that oscillations with a period comparable to the penetration time appear to be largely absent. If substantial oscillations with this period were seen the assumption of a steady one-dimensional magnetopause model would be invalid.

Finally, it is noted that the average magnetic-field component normal to the magnetopause undergoes a systematic change from negative values (i.e., pointing towards the earth) to positive ones for the successive boundary penetrations in the time period 19.21 - 19.38 UT. A possible interpretation of this observation will be presented in the discussion section. Normal field components of a magnitude greater than about 5γ should be considered as significant.

Discussion

The minimum-variance analysis discussed in the previous section has led to the following conclusions concerning the five Explorer 12 boundary penetrations on Sept. 24, 1961, 19.21 - 19.40 UT:

i) The magnetic field component perpendicular to the magnetopause is negative, i.e., it points towards the earth during the first boundary penetration (19.21 UT). For the subsequent penetrations the normal field component first approaches zero. It then takes on a large positive value, i.e., it points away from the earth, during the final penetration (19.38 UT).

ii) The polarization of the magnetopause current layer also changes in a systematic manner during the period 19.21 - 19.40 UT, as shown by Figures 8 - 12. The sense of rotation of the magnetic field vector seen by an observer facing the sun and travelling outwards through the current layer is right-hand for the boundary at 19.21 UT and left-hand for the one at 19.38 UT. For the intermediate boundaries the sense is undefined.

It is proposed here that these observations are compatible with the so-called open magnetosphere model (Dungey, 1961, Levy et al, 1964). The main feature of this field model is an X-type null line in the field intensity on the front side of the magnetospheric surface. This line is formed between the transition zone field, assumed to be due south, and the

geomagnetic field which is due north. If these two fields are not exactly antiparallel there will be a field component along the "null" line so that the field intensity is not strictly zero there. At the null line the process of magnetic field reconnection takes place. In the region north of the null line the magnetic-field component perpendicular to the magnetospheric surface points inwards while south of that line it points outwards. The magnitude of this normal-field component is substantial; theoretical studies (Levy et al, 1964) suggest a value of 10 - 20% of the total field.

If the open model is adopted for the purposes of interpreting the Sept. 24 event it is found that the satellite must have been north of the null line at 19.21 UT and south of it at 19.38 UT. It is noted that the null line in the open model should pass through the forward stagnation point in the solar-wind flow past the magnetosphere and that it should lie in the vicinity of the solar-magnetospheric equatorial plane when the transition-zone field is nearly antiparallel to the geomagnetic field as was the case for the Sept. 24 event. But it was pointed out in the introduction that the satellite was located extremely near the solar magnetospheric equatorial plane during the time 19.21 - 19.40 UT. Even though the satellite was in fact slightly south of that plane at 19.21 UT and slightly north of it at 19.40 UT it is reasonable to assume that the null line could have moved around in such a manner that the satellite was in fact slightly north of the null line at 19.21 UT and slightly

south of it at 19.38 UT. The motion required for this is minute.

A second feature of the open magnetosphere model is that away from the null line, the change in field direction at the magnetopause is accomplished by a so-called rotational discontinuity (Levy et al, 1964). This discontinuity is a large amplitude Alfvén wave, which in the magnetospheric application propagates into the transition zone with the Alfvén speed based on the component of the magnetic field perpendicular to the wave front. At the same time it is swept back towards the magnetosphere at the same speed by the transition-zone plasma flow. Thus, a standing wave front, the magnetopause, results. In the magnetohydrodynamic approximation the rotational discontinuity has the property that the field magnitude is preserved while the field direction changes. Since the normal field component must be conserved across the discontinuity it follows that in the discontinuity the field component tangential to the magnetopause must rotate from the magnetospheric direction to the transition-zone direction under conservation of its magnitude, hence the name rotational discontinuity.

Examination of Figures 12 and 13 shows that the observed behavior of the magnetopause field at 19.38 UT is indeed compatible with this structure. The magnetic-field component normal to the magnetopause is substantial (Fig. 13) and the tangential-field component remains approximately constant as its direction changes (Fig. 12). Over the entire time period

of this boundary the field magnitude does change substantially as shown in Fig. 2d. In the flow model proposed by Levy et al, (1964), the field-magnitude changes at the magnetopause in general occur somewhat closer to the earth than the field direction changes. While this tendency appears to be present in Fig. 2d there is a substantial overlap between the regions in which the field-direction and the field-magnitude changes occur. This may be due to the proximity of the null line where the two regions are expected to merge. Fluctuations in field magnitude, presumably due to compression waves travelling across the magnetopause, or to field irregularities convected across it, are also apparent in Fig. 2d. (Further comments on the possibility of a nonconstant magnetic field in a rotational discontinuity are found in Su and Sonnerup, 1968; Gerdin and Sonnerup, 1969; and in Hudson, 1970.)

Turning next to the boundary at 19.21 UT (Fig. 8) it is apparent that the field magnitude does not remain constant; there is a pronounced minimum in the middle of the current layer. Normally a structure of this type would be interpreted as a tangential discontinuity or a sheet pinch and it would be associated with the closed magnetosphere model. However, as pointed out previously, there is a substantial magnetic-field component perpendicular to the layer and this renders the interpretation of the layer as a tangential discontinuity invalid. Again it is proposed that the field magnitude variation is due to the proximity of the null line. If the polarization of the

magnetopause current layer changes at the null line as suggested by the present observations (when interpreted in the context of the open magnetopshere model) then the field component B_2 along the $\underset{\sim}{n}_2$ axis must change sign at the null line. This implies that a magnetopause penetration near the null line may yield a polar plot of the type shown in Fig. 8.

In brief, the 19.21 UT boundary is interpreted as a rotational discontinuity located slightly north of the null line and modified by its close proximity to that line. Since the 19.38 UT boundary occurred on the southern side of the null line, the intermediate boundaries (at 19.25.30, 19.26.00 and 19.27.30 UT) would then represent the magnetopause structure at, or extremely near, the location of the null line itself. The extremely weak magnetic field in the time interval between the 19.25.30 and the 19.26.00 UT boundaries suggests that the satellite may in fact have penetrated into the magnetopause very near the null line and that it did not emerge completely on the transition-zone side of the magnetopause. In the 19.27.30 UT boundary a complete penetration took place. The behavior of the tangential-field component in this case (Fig. 11) is remarkable. In the early portion of the penetration there is a tendency for the polarization to agree with the one on 19.21 UT (Fig. 8) while in the late portion there is a tendency towards agreement with the 19.38 UT case (Fig. 12).

If one adopts the interpretation of the two boundaries at 19.21 UT and at 19.38 UT as rotational discontinuities, i.e.,

as standing Alfvén waves, then it becomes clear that the observed polarization change of the magnetopause current layer, mentioned earlier, should be related to the polarization of the Alfvén wave. Since the magnetic field component perpendicular to the magnetopause is opposite at 19.21 UT and at 19.38 UT, one concludes that the polarization of the magnetopause viewed as an Alfvén wave is the same for both boundaries, and that it is the same as for the electron-whistler mode.

Observations of opposite senses of rotation of the tangential field component at magnetopause above and below the solar magnetospheric equatorial plane have been reported previously (Sonnerup and Cahill, 1968) and the senses observed were in agreement with the interpretation of the magnetopause as an electron-polarized Alfvén wave. However, the sign and magnitude of the magnetic field component normal to the magnetopause were not available for most of the boundaries contained in that study. It is also noted that a theoretical explanation of the absence of the proton polarization has been given by Su and Sonnerup, (1968).

In summary, it appears that the Explorer 12 magnetometer observations from the Sept. 24, 1961 reentry into the magnetosphere are explained in considerable detail by the so-called open model or reconnection model of the magnetosphere. In addition to explaining the observed normal-field components and their relationship to the observed polarization change of the magnetopause, this model would also account for the fact

that on this occasion the magnetopause appeared capable of transmitting compressive waves or frozen-in field structures from the transition zone into the magnetosphere. (See Figures 2a and 2b.) This is usually not observed (Kaufmann, 1970). There is theoretical evidence that a magnetopause boundary of the tangential-discontinuity type associated with the so-called closed magnetosphere might be an effective reflector of such waves (McKenzie, 1970). For an open magnetosphere model the plasma conditions on both sides of the magnetopause would be similar and one would expect the transmission coefficient to be high. Also, magnetic-field variations frozen in the transition-zone plasma can readily be convected across the magnetopause in the open model. Finally, the closed magnetosphere model would require the normal-field components calculated here to be spurious. This appears unlikely, in particular for the 19.38 UT boundary.

In closing it is worth emphasizing that the observations presented here represent a single event which occurred during a magnetic storm. Thus it is not possible to infer from the interpretation proposed here that the open magnetosphere model is always applicable. Indeed, it is likely that this model occurs only for brief periods of time and only in connection with certain types of geomagnetic disturbances, and that under normal circumstances the closed magnetosphere model is valid (see, e.g., Sonnerup and Cahill, 1967).

Acknowledgement

The author wishes to thank Dr. L.J. Cahill, Jr., of the University of Minnesota, for the use of the Explorer 12 data and for arranging the improved data-reduction procedure. Several helpful discussions with Dr. R.L. Kaufmann of the University of New Hampshire are gratefully acknowledged.

The research was supported by the National Aeronautics and Space Administration under Grants NGR-30-001-011 to Dartmouth College, and NSG-624 to the University of New Hampshire.

References

Cahill, L.J., Jr., and P.G. Amazeen, The boundary of the geomagnetic field, J. Geophys. Res., 68, 1835, 1963.

Davis, L.R., and A. Konradi, Response of the ion-electron detector flown on Explorer 12 August to December, 1961, Goddard Space Flight Center Report X-612-68-447, 1968.

Dungey, J.W., Interplanetary magnetic field and the auroral zone, Phys. Rev. Letters, 6, 47, 1961.

Gerdin, G.A., and B.U.Ö. Sonnerup, Nature of the rotational discontinuity, Phys. Fluids, 12, 145, 1969.

Hudson, P.D., The classification of solar wind discontinuities, Preprint, Physics Department Imperial College of Science and Technology, London, 1970.

Kaufmann, R.L., J.-T. Horng, and A. Wolfe, Large amplitude hydromagnetic waves in the inner magnetosheath, to appear: J. Geophys. Res., 75, Sept., 1970.

Levy, R.H., H.E. Petschek, and G.L. Siscoe, Aerodynamic aspects of the magnetospheric flow, AIAA J., 2, 2065, 1964.

McKenzie, J.F., Hydromagnetic wave interaction with the magnetopause and the bow shock, Planet. Space Sci., 18, 1, 1970.

Sonnerup, B.U.Ö., and L.J. Cahill, Jr., Magnetopause structure and attitude from Explorer 12 observations, J. Geophys. Res., 72, 171, 1967.

Sonnerup, B.U.Ö., and L.J. Cahill, Jr., Explorer 12 observations of the magnetopause current layer, J. Geophys. Res., 73, 1757, 1968.

Su, S.-Y., and B.U.Ö. Sonnerup, First-order orbit theory of the rotational discontinuity, Phys. Fluids, 11, 851, 1968.

Figure Captions

Fig. 1. Magnetograms from several low and mid-latitude stations showing the time variation of the horizontal magnetic field component during the magnetic storm of Sept. 24, 1961.

Fig. 2. Survey plots of the Explorer 12 magnetic-field observations during the period 19.15 - 19.46 UT on the inbound pass of Sept. 24, 1961. The field is presented in terms of the field magnitude, B, and two angles α and ψ giving the orientation of the field vector relative to the satellite spin axis and the plane containing the spin axis and the sun direction. Magnetopause penetrations are seen at 19.21, 19.25.30, 19.26, 19.27.30 and 19.38 UT.

Fig. 3. Detailed record of the magnetopause penetration at 19.21 UT.

Fig. 4. Detailed record of the magnetopause penetration at 19.25.30 UT.

Fig. 5. Detailed record of the magnetopause penetration at 19.26 UT.

Fig. 6. Detailed record of the magnetopause penetration at 19.27.30 UT.

Fig. 7. Detailed record of the magnetopause penetration at 19.38 UT.

Fig. 8. Polar plot of the magnetic-field component tangential to the magnetopause surface for the penetration at 19.21 UT. The directions (2) and (3) correspond to the vectors $\underset{\sim}{n}_2$ and $\underset{\sim}{n}_3$ in Table 2.

Fig. 9. Polar plot of the magnetic-field component tangential to the magnetopause surface for the penetration at 19.25.30 UT. The directions (2) and (3) correspond to the vectors $\underset{\sim}{n}_2$ and $\underset{\sim}{n}_3$ in Table 2.

Fig. 10. Polar plot of the magnetic field component tangential to the magnetopause surface for the penetration at 19.26 UT. The directions (2) and (3) correspond to the vectors $\underset{\sim}{n}_2$ and $\underset{\sim}{n}_3$ in Table 2.

Fig. 11. Polar plot of the magnetic field component tangential to the magnetopause surface for the penetration at 19.27.30 UT. The directions (2) and (3) correspond to the vectors $\underset{\sim}{n}_2$ and $\underset{\sim}{n}_3$ in Table 2.

Fig. 12. Polar plot of the magnetic field component tangential to the magnetopause surface for the penetration at 19.38 UT. The directions (2) and (3) correspond to the vectors $\underset{\sim}{n}_2$ and $\underset{\sim}{n}_3$ in Table 2. The vector B_i denotes the field direction on the magnetosphere side of the magnetopause at 19.45 UT.

Fig. 13. Time variation of the magnetic field component normal to the magnetopause current layer.

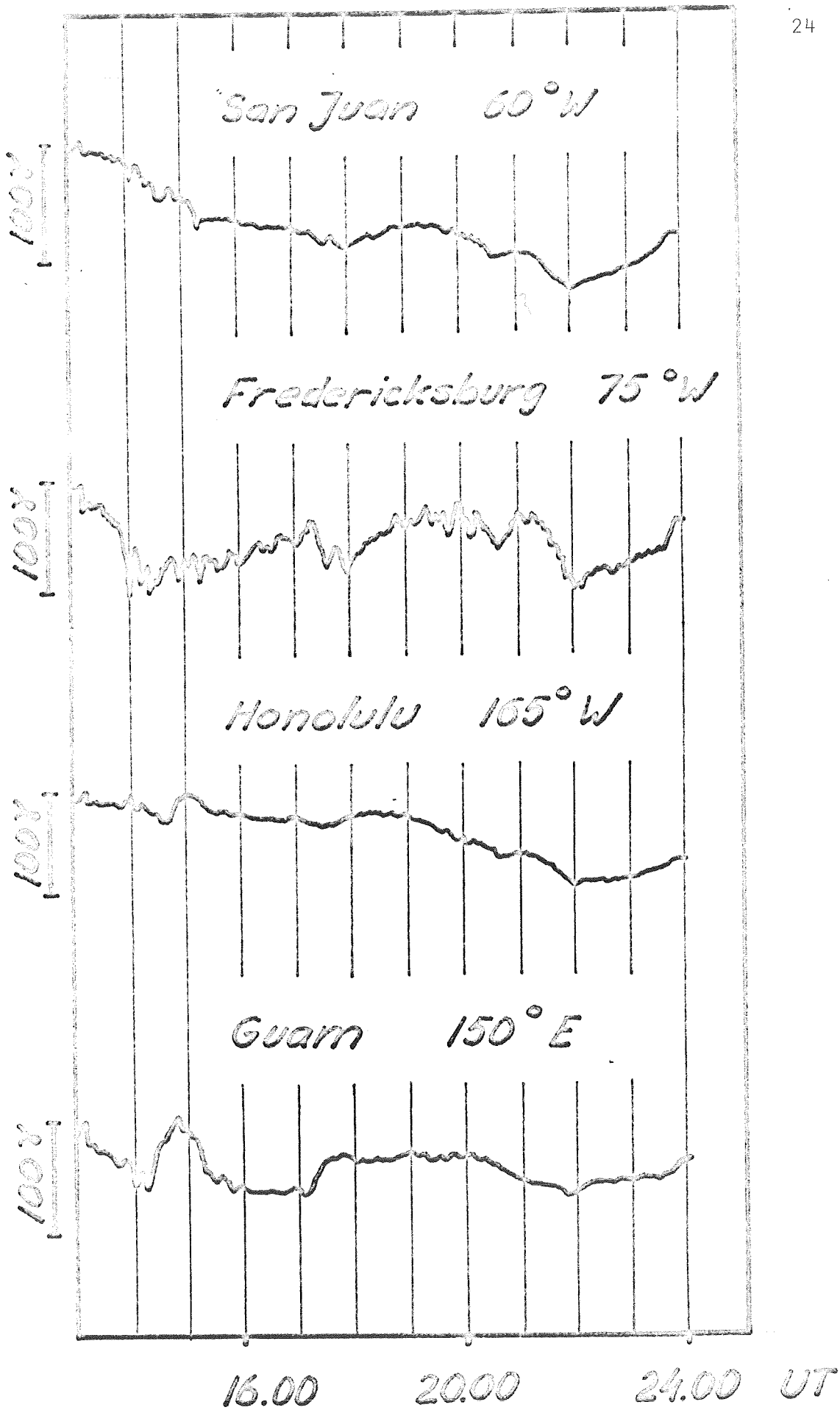
San Juan 60°W
100γ
Fredericksburg 75°W
100γ
Honolulu 165°W
100γ
Guam 150°E
100γ
16.00
20.00
24.00 UT

Fig. 1

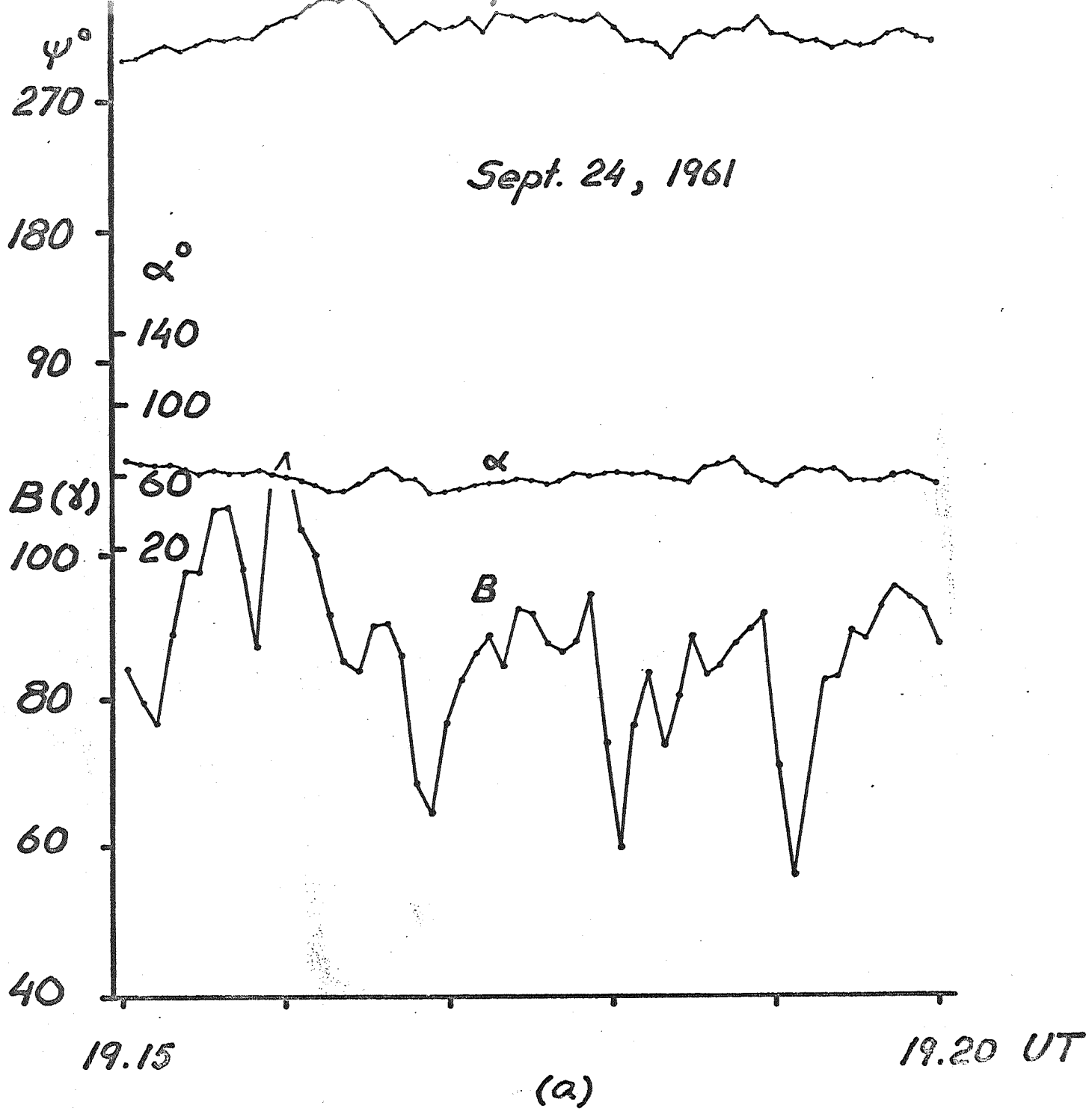
ψ°
270
Sept. 24, 1961
180
α°
140
90
100
α
60
B(γ)
20
100
B
80
60
40
19.15
19.20 UT
(a)

Fig. 2a

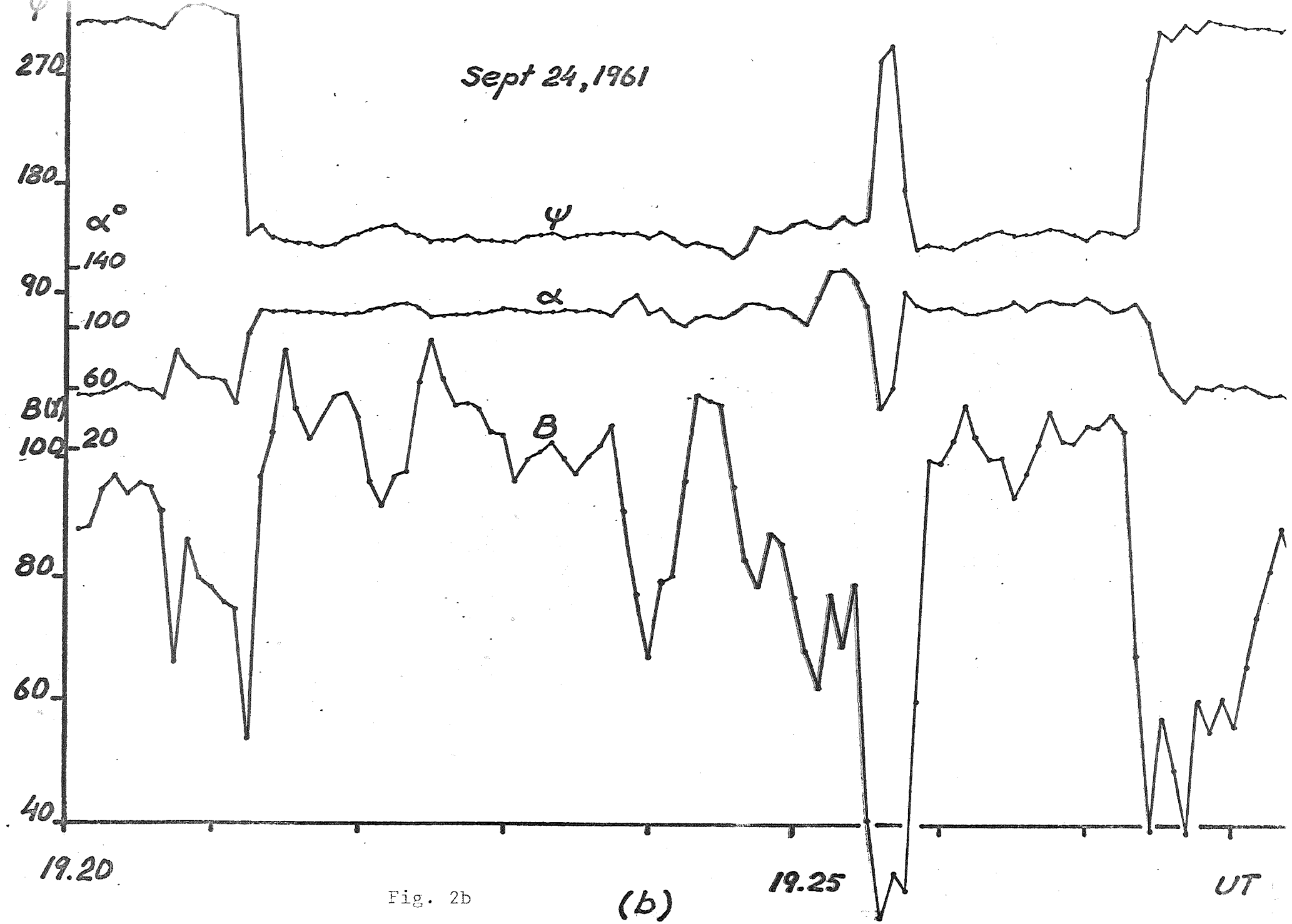
Sept 24, 1961
270
180
90
60
40
α°
140
100
20
B(γ)
100
80
60
40
Ψ
α
B
19.20
19.25
UT

Fig. 2b

(b)

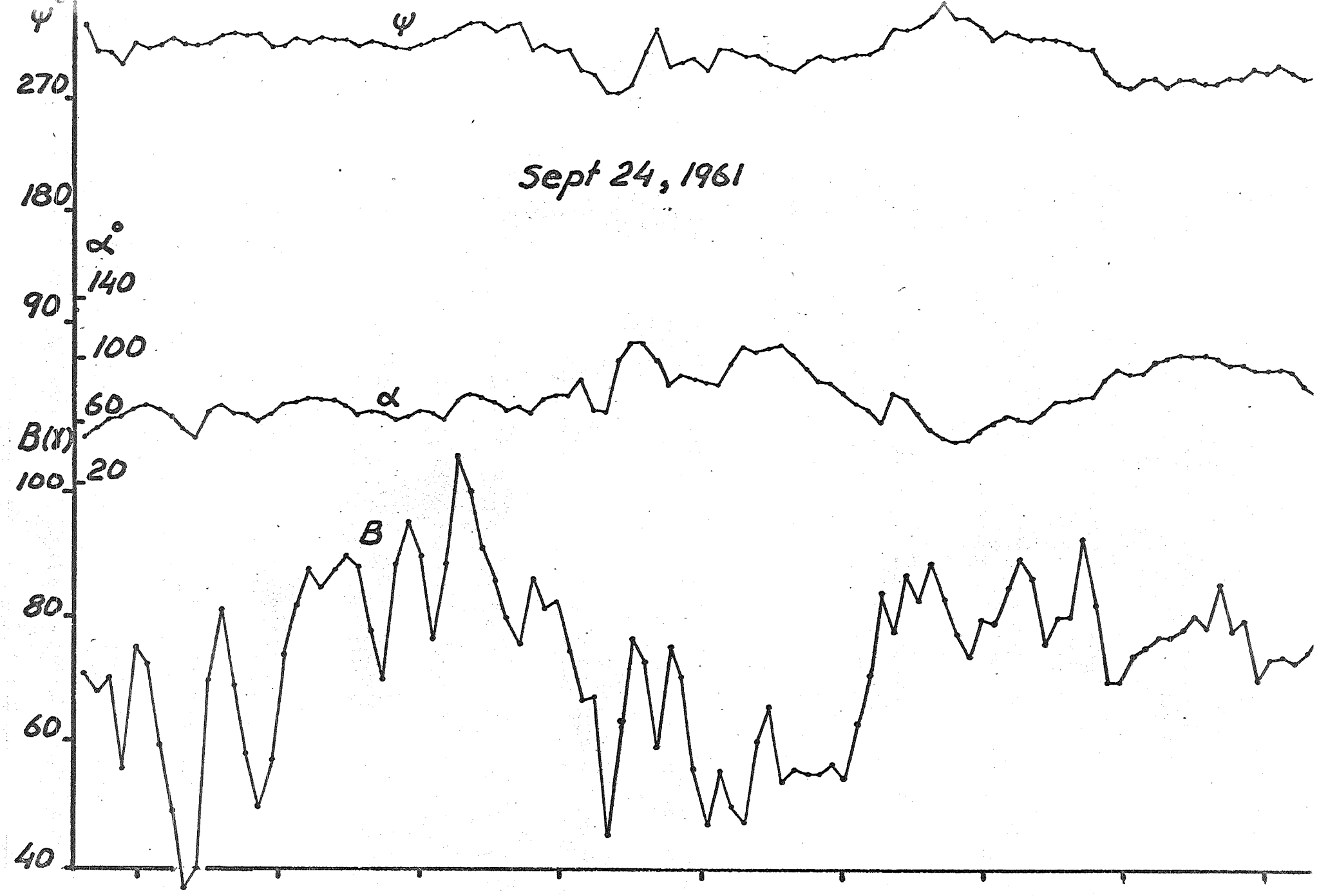
ψ
270
180
Sept 24, 1961
α°
140
90
100
60
α
B(γ)
100
20
B
80
60
40
19.30
19.35
UT

Fig. 2c

(c)

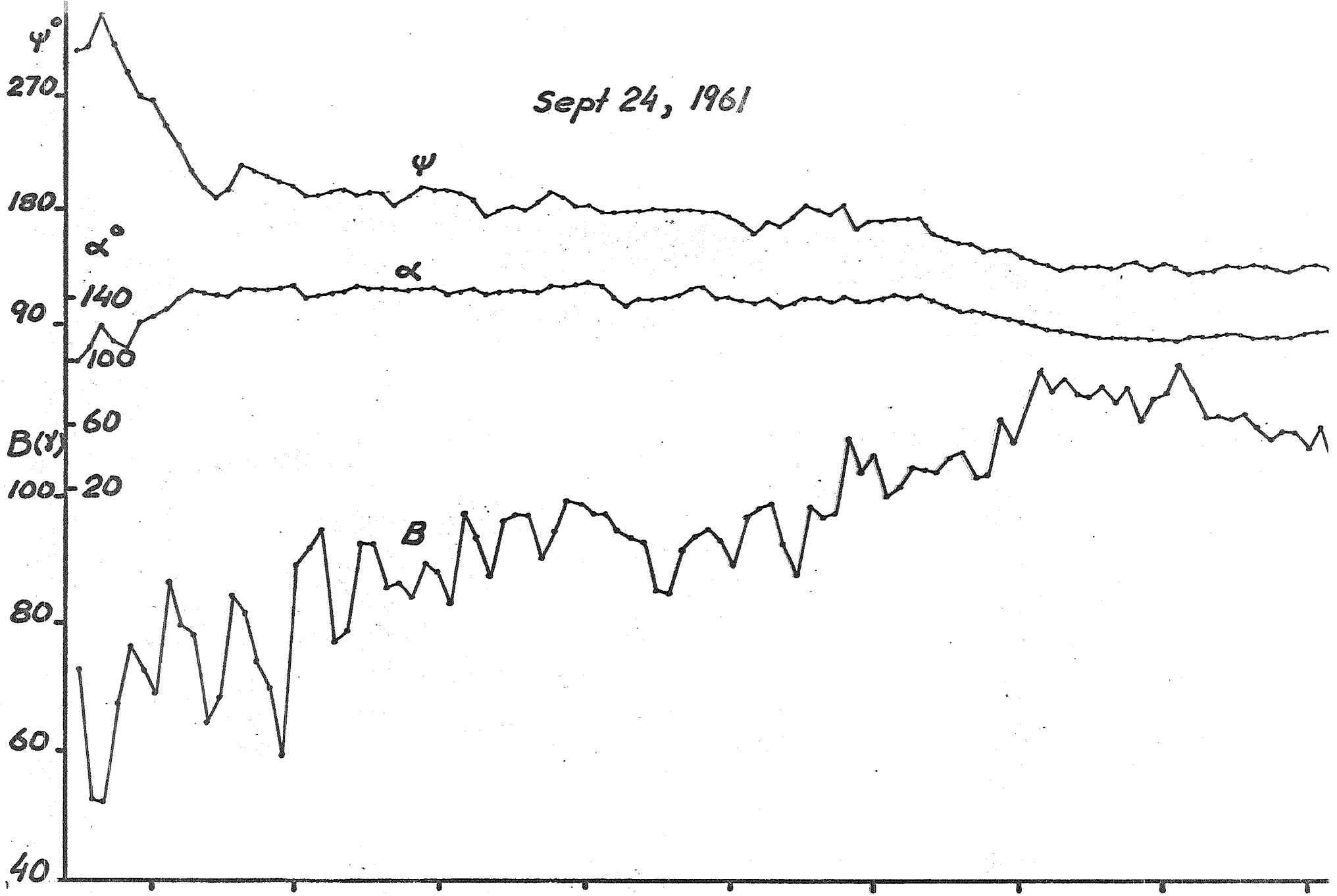
Sept 24, 1961
ψ°
270
180
ψ
α°
140
90
α
100
60
B(γ)
100
20
B
80
60
40
19.40
19.45 UT

Fig. 2d

(d)

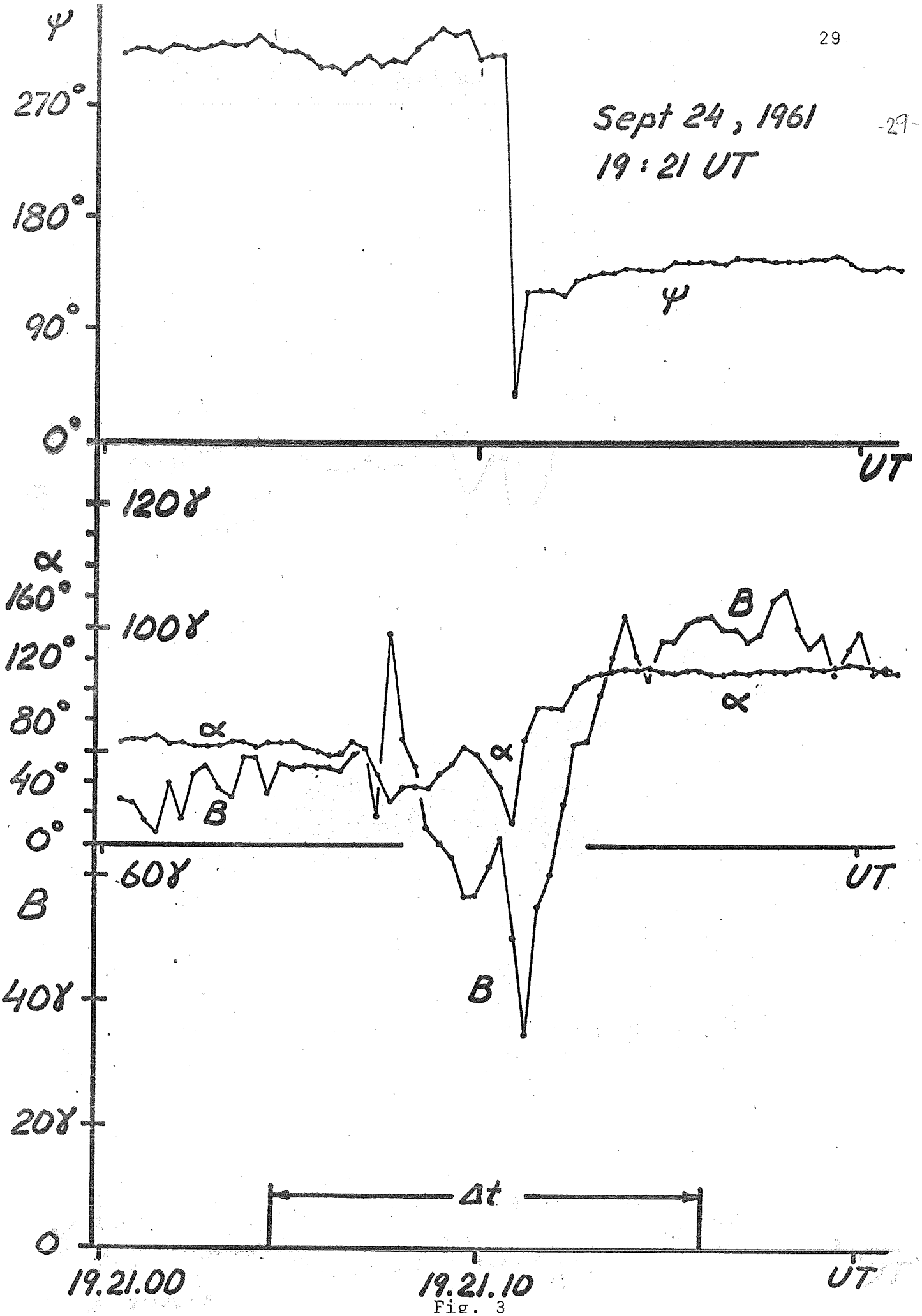
ψ
270°
180°
90°
0°
UT
Sept 24, 1961
19:21 UT
ψ
120γ
α
160°
100γ
120°
80°
40°
0°
60γ
B
40γ
20γ
0
α
B
B
α
B
α
UT
Δt
19.21.00
19.21.10
UT

Fig. 3

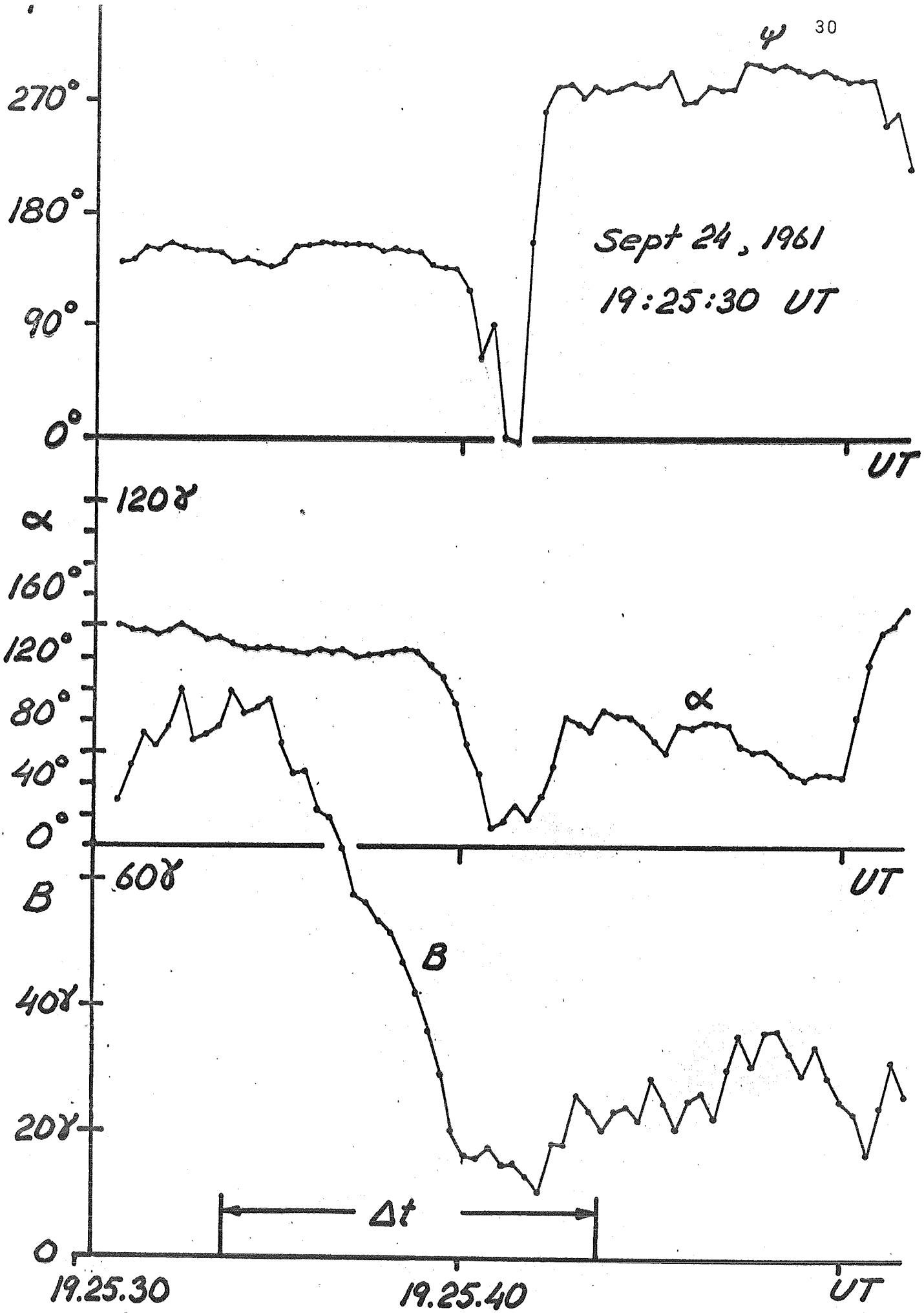
ψ
270°
180°
90°
0°
UT
Sept 24, 1961
19:25:30 UT
120γ
α
160°
120°
80°
40°
0°
α
UT
60γ
B
B
40γ
20γ
0
Δt
19.25.30
19.25.40
UT

Fig. 4

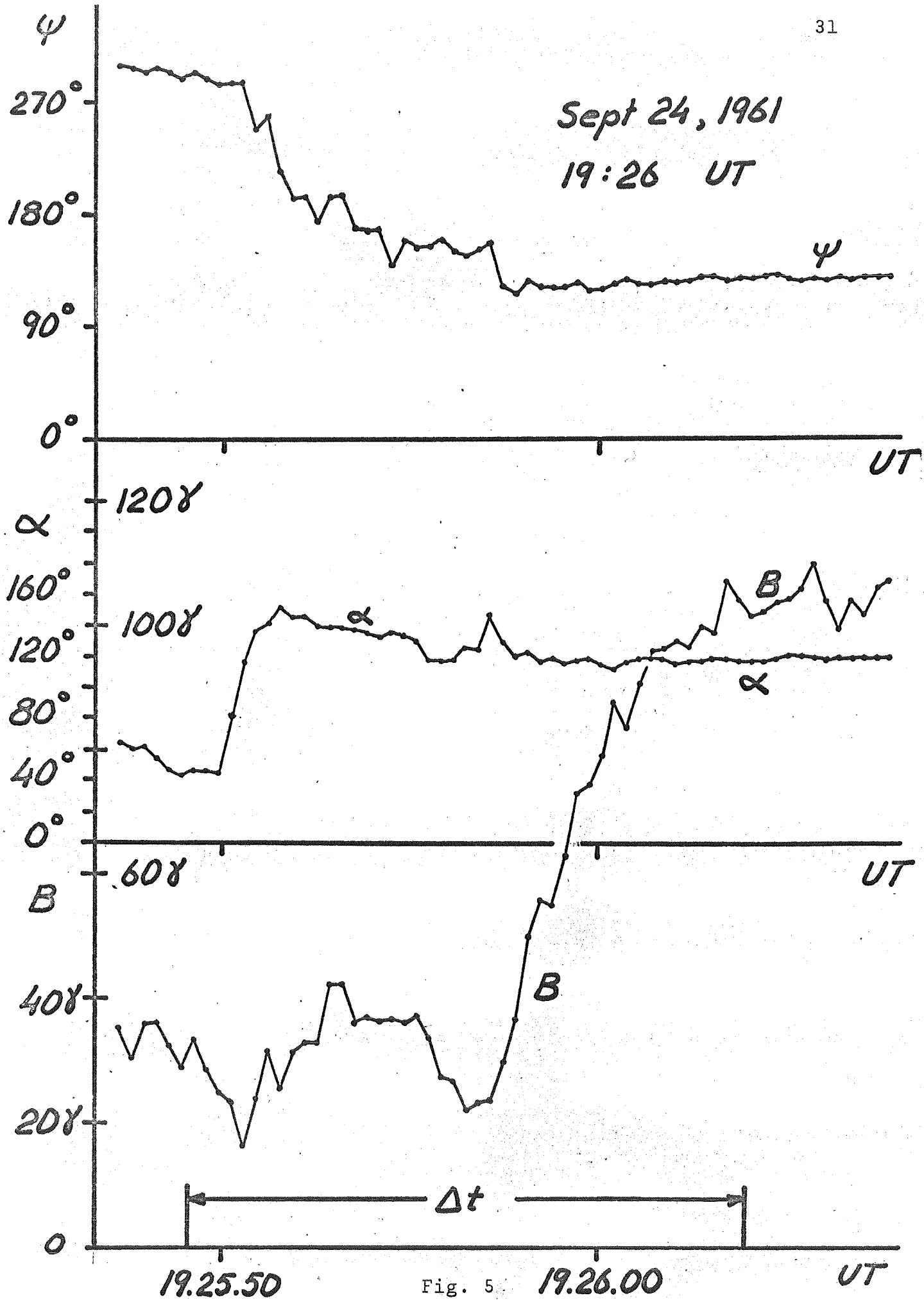
ψ
270°
180°
90°
0°
Sept 24, 1961
19:26 UT
ψ
UT
120γ
α
160°
100γ
120°
80°
40°
0°
B
α
α
UT
60γ
B
40γ
B
20γ
0
Δt
19.25.50
19.26.00
UT

Fig. 5

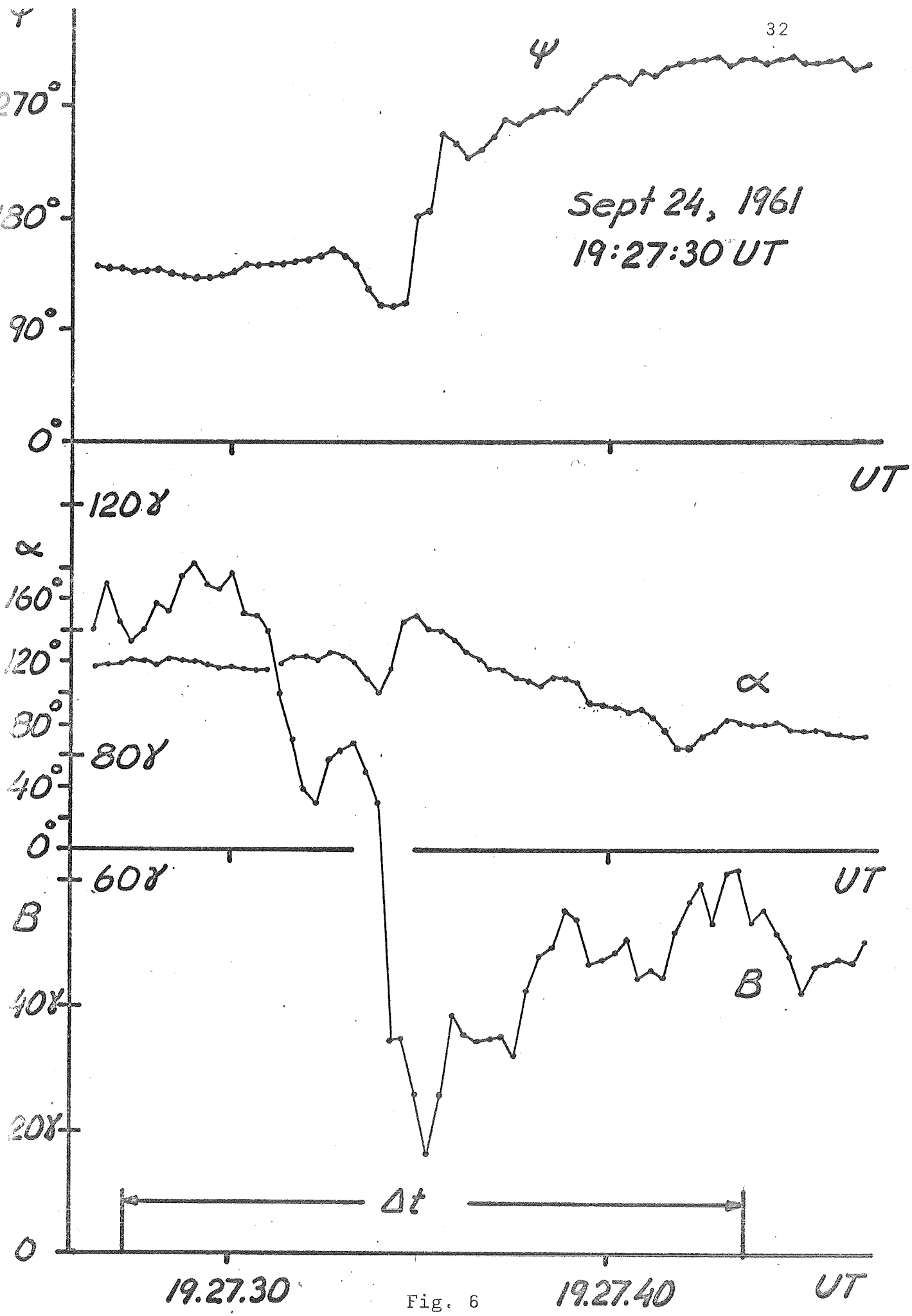
ψ
270°
180°
90°
0°
Sept 24, 1961
19:27:30 UT
UT
120γ
α
160°
120°
80°
40°
0°
80γ
60γ
α
UT
B
40γ
20γ
0
B
Δt
19.27.30
19.27.40
UT

Fig. 6

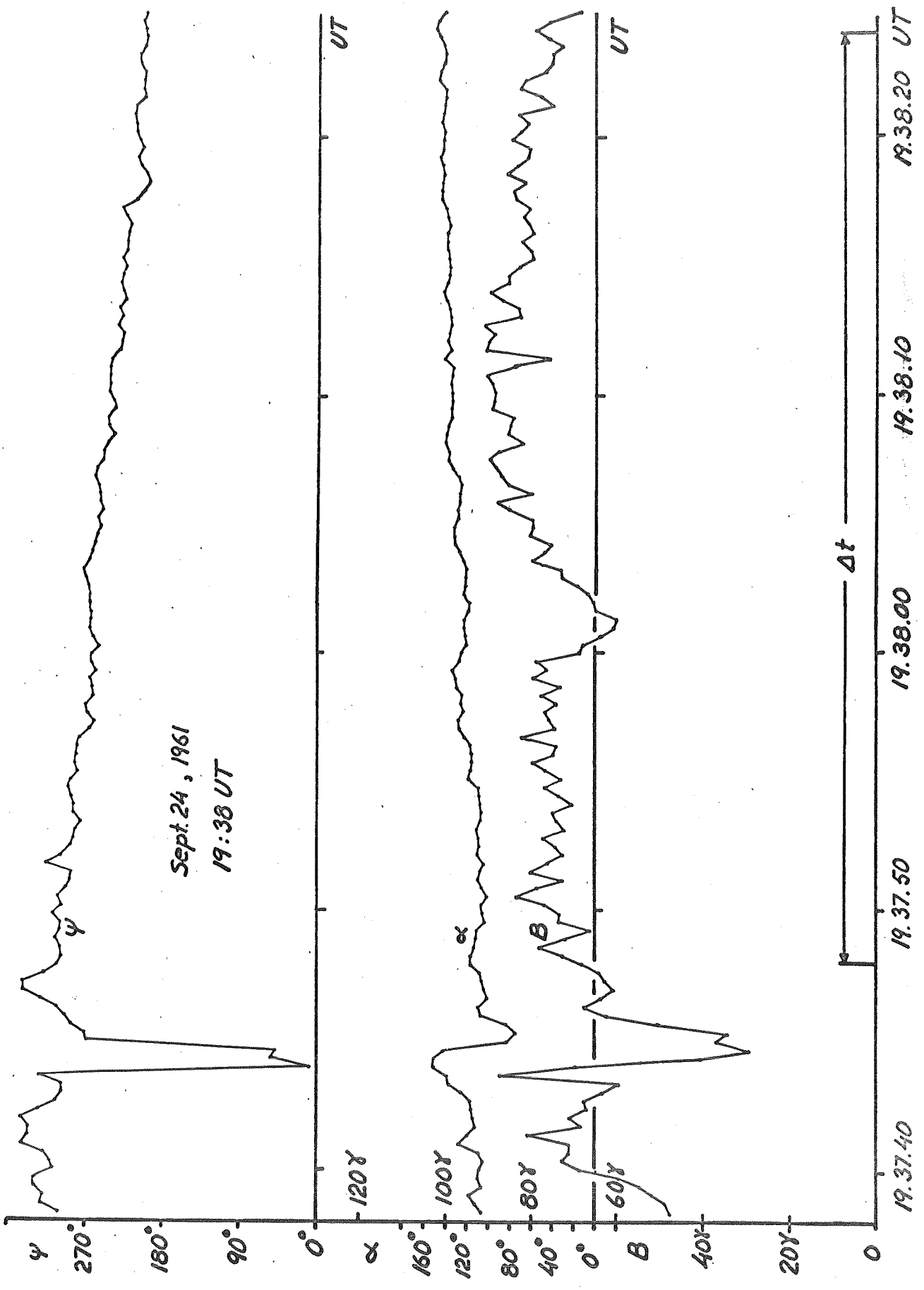
ψ
270°
180°
90°
0°
ψ
Sept. 24, 1961
19:38 UT
UT
α
120γ
160°
120°
80°
40°
0°
100γ
80γ
60γ
α
β
β
40γ
20γ
0
Δt
19.37.40
19.37.50
19.38.00
19.38.10
19.38.20
UT

Fig. 7

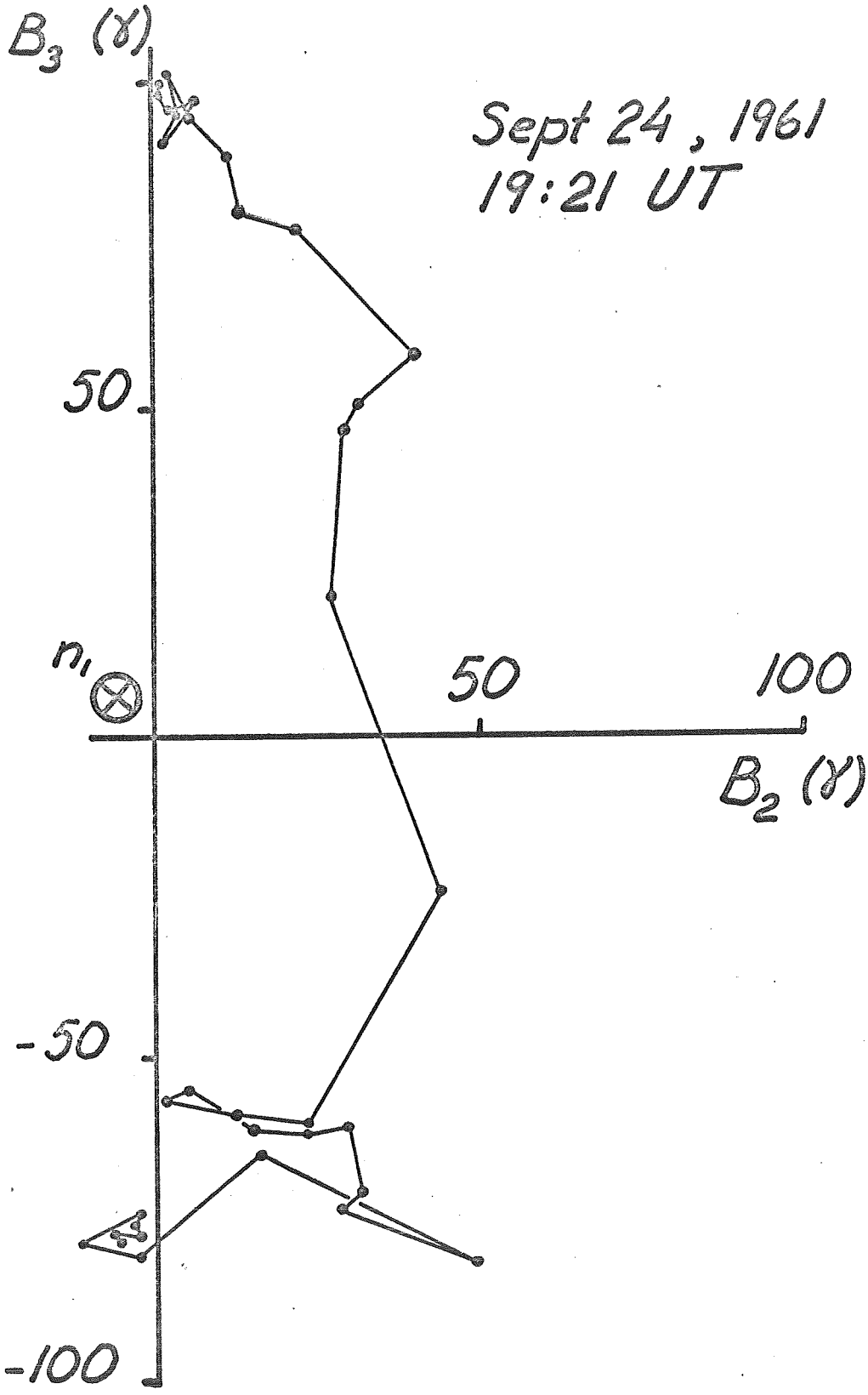

Fig. 8

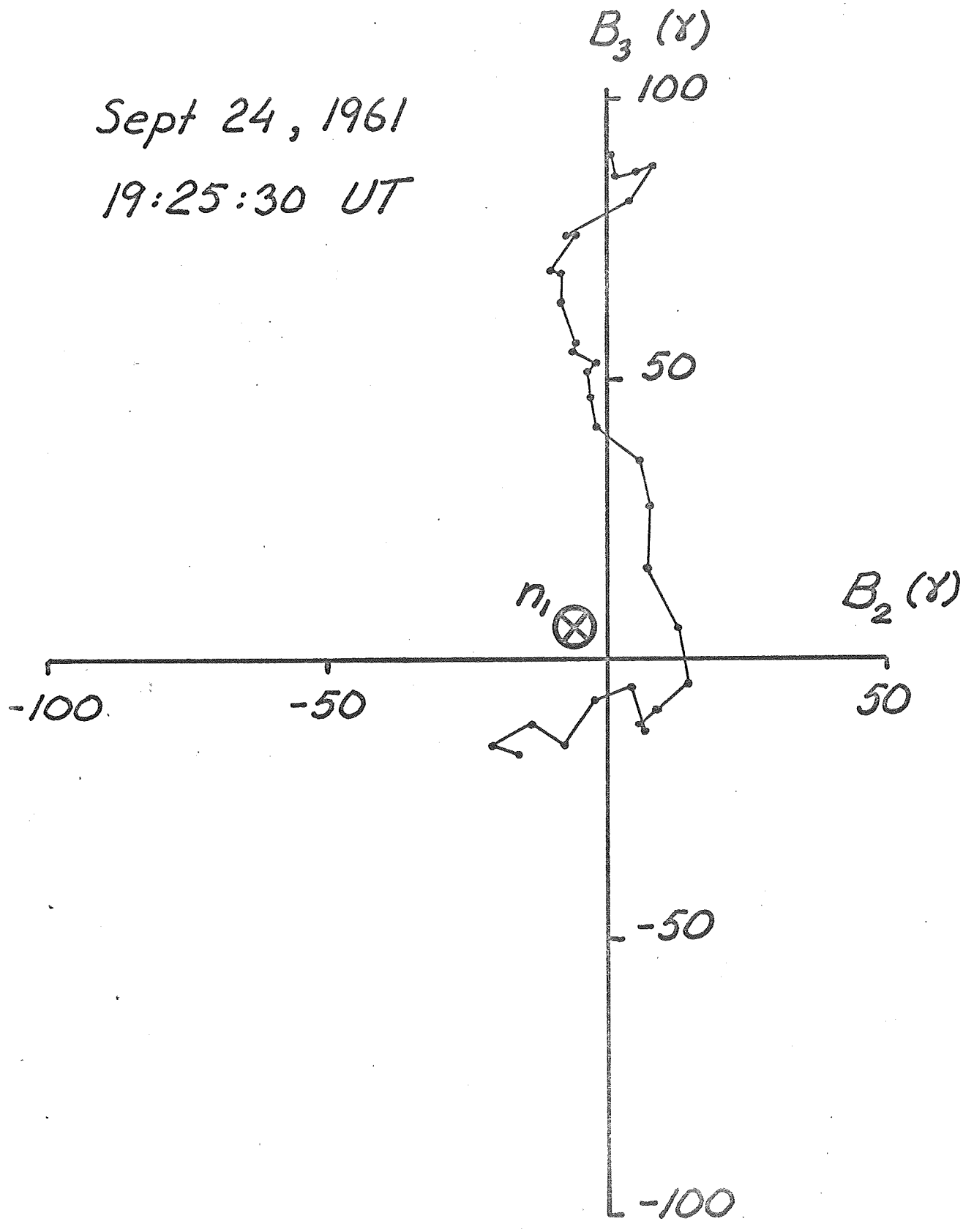

Fig. 9

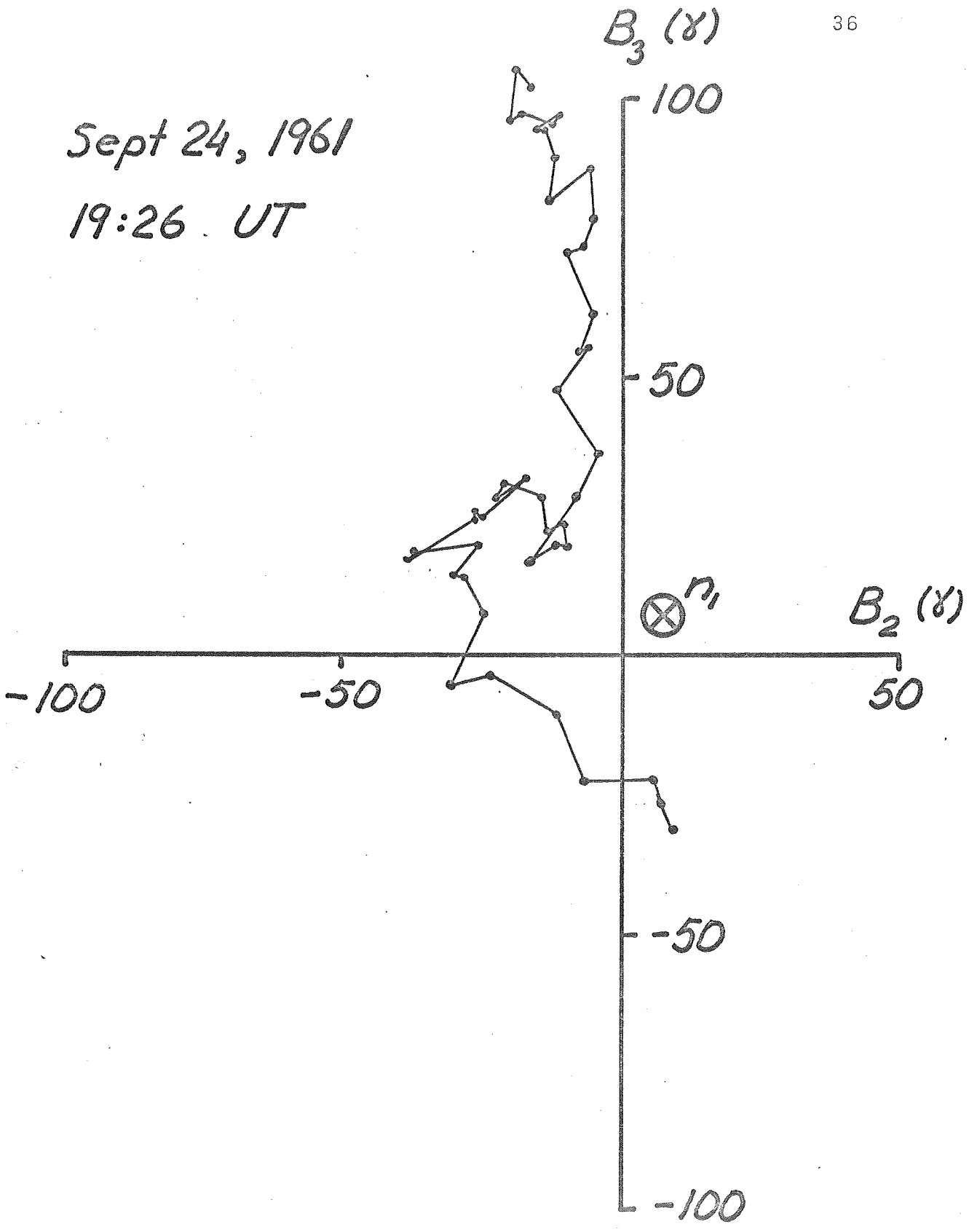

Fig. 10

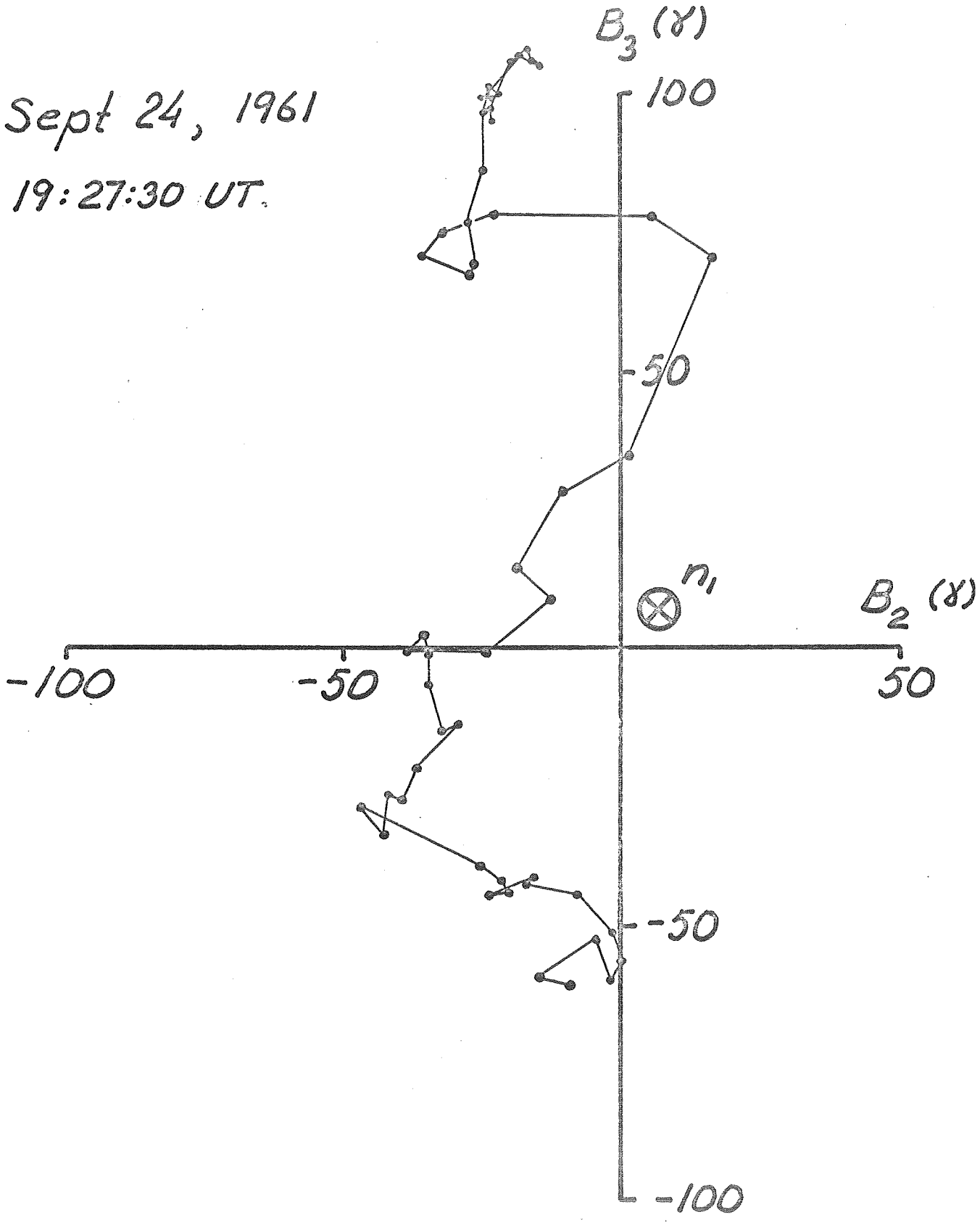

Fig. 11

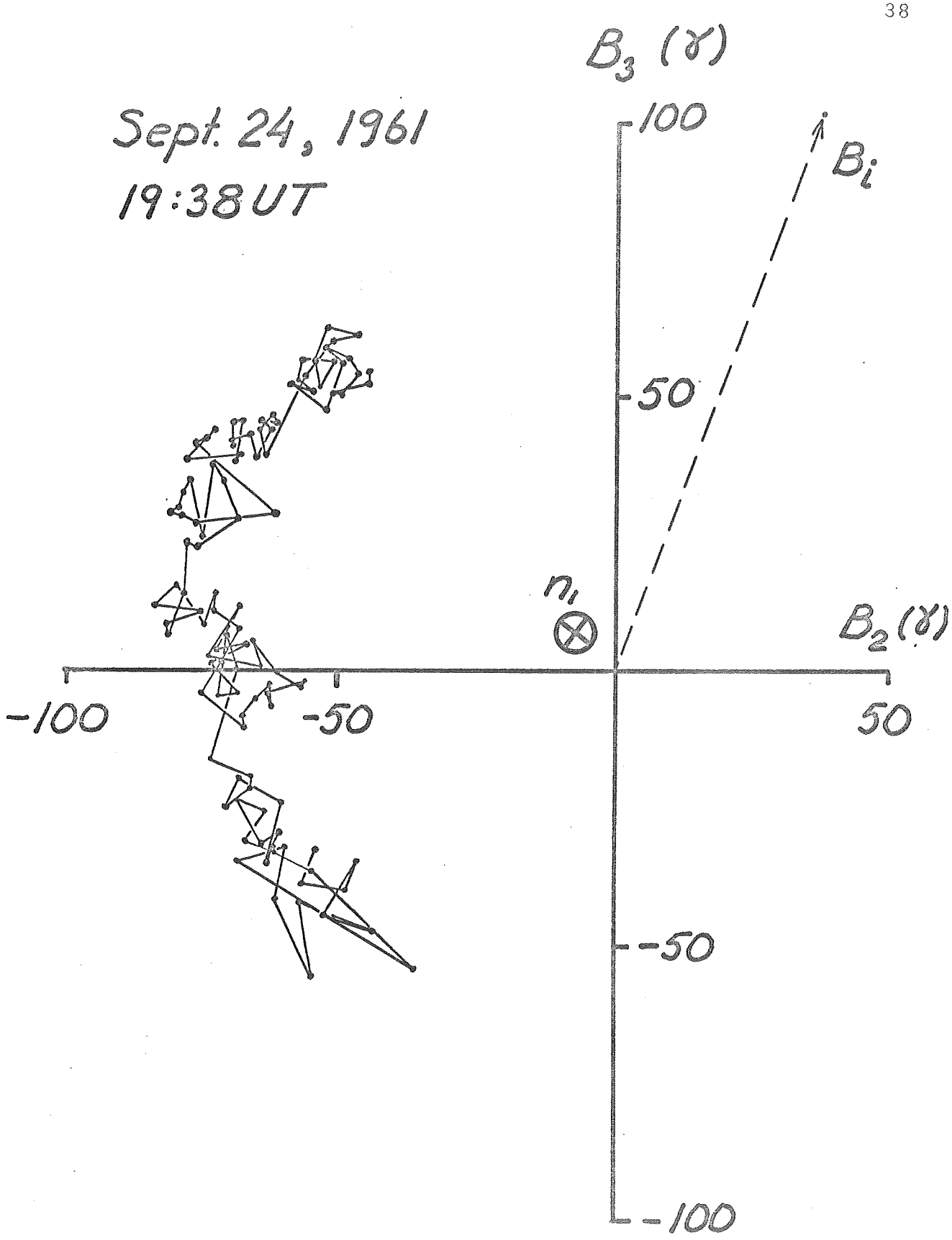

Fig. 12

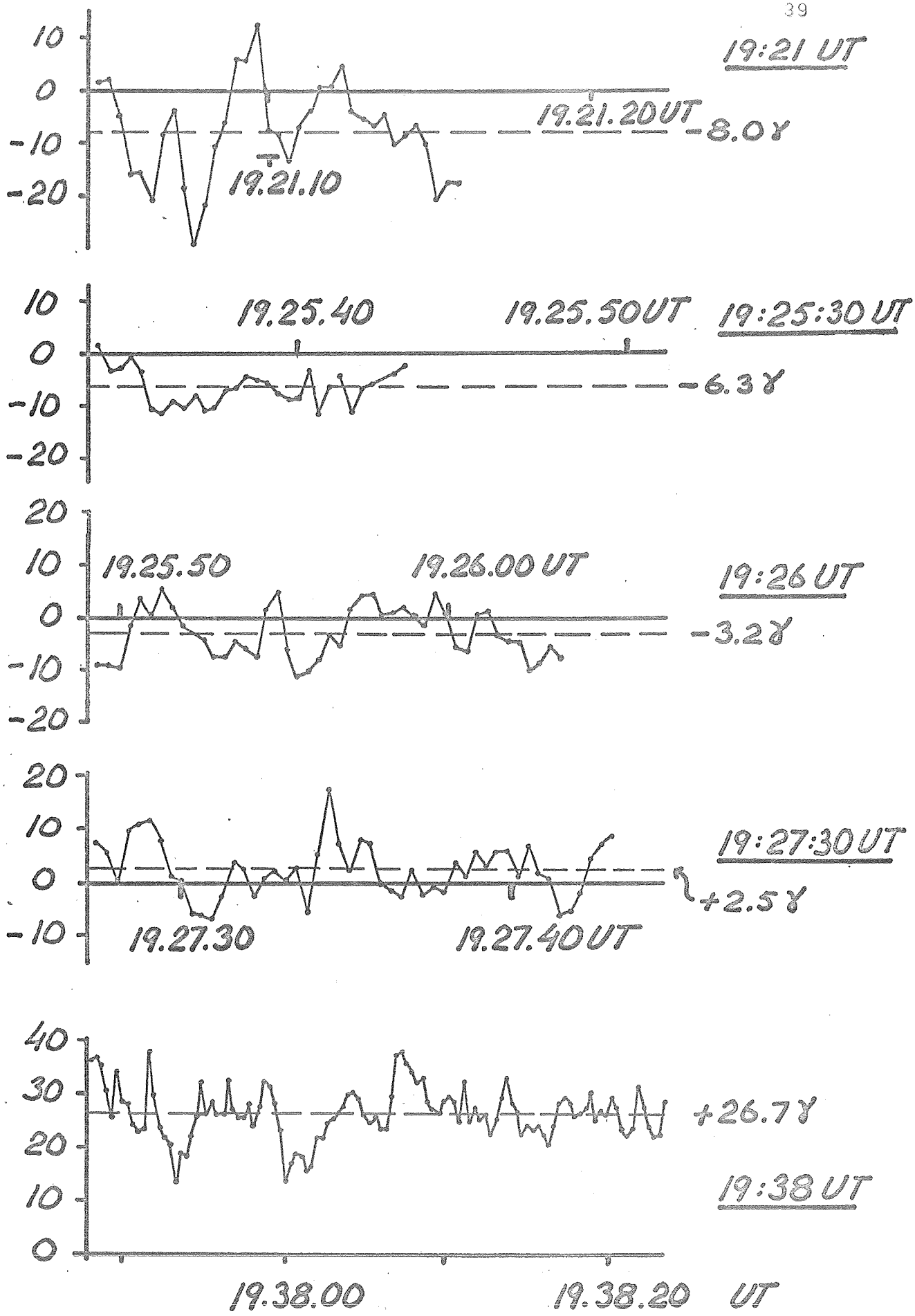
B·n (γ)
Sept 24, 1961
10
0
-10
-20
19:21 UT
19.21.20 UT
-8.0γ
19.21.10
10
0
-10
-20
19.25.40
19.25.50 UT
19:25:30 UT
-6.3γ
20
10
0
-10
-20
19.25.50
19.26.00 UT
19:26 UT
-3.2γ
20
10
0
-10
19:27:30 UT
+2.5γ
19.27.30
19.27.40 UT
40
30
20
10
0
+26.7γ
19:38 UT
19.38.00
19.38.20 UT

Fig. 13